Available online at www.sciencedirect.com
ScienceDirect
Journal of Magnetic Resonance 185 (2007) 183–190
JMR Journal of Magnetic Resonance
www.elsevier.com/locate/jmr

Diffraction-like phenomena in a periodic magnetization distribution at 1.5 T using the distant dipolar field (DDF)

Stefan Kirsch, Peter Bachert *

Department of Medical Physics in Radiology, German Cancer Research Center (dkfz), D-69120 Heidelberg, Germany

Received 21 July 2006; revised 28 September 2006
Available online 15 November 2006

Abstract

In the CRAZED experiment (COSY revamped by asymmetric Z-gradient echo detection, Warren et al.), a spatially anisotropic magnetization distribution is created by application of a magnetic field gradient (strength G, duration τ) which in turn generates a response called the distant dipolar field (DDF). The DDF is a source of intermolecular multiple-quantum coherences (iMQC) which contain information on the distance $d = \pi/(\gamma G\tau)$ between pairs of dipolar-coupled spins. Diffraction-like phenomena may result for periodically structured samples. In this study, we report the observation of diffraction owing to the DDF at 1.5 T using a clinical whole-body tomograph. Based on the semi-classical treatment of the problem by Robyr and Bowtell, diffraction conditions were obtained for a CRAZED-type pulse sequence that selects iMQC of order N. The predicted distinct difference in $N = 2$ and $N \neq 2$ coherences, i.e., a dominant continuous course as a function of τ ($N = 2$) and prominent diffraction peaks otherwise, could be verified in CRAZED experiments in a periodically structured sample selecting coherence orders $N = 2$ and $N = 3$. The diffractive signal component contains information on the geometric structure of the sample. Applications of this technique may permit the detection of changes in composition and geometry of periodic structures.

Keywords: CRAZED; Distant dipolar field (DDF); Intermolecular multiple-quantum coherence; Diffraction

1. Introduction

The temporal evolution of the nuclear magnetization in NMR experiments on liquids is well described by the Bloch equations. The macroscopic magnetization is generated by the nuclear spins of the sample, which are assumed to evolve without mutual static coupling. Interestingly, while short-range dipole–dipole interactions average to zero due to molecular tumbling motion, and thus satisfy this assumption, the long-range dipole–dipole interactions remain. These are the cause for an observable response of the spin system, called the distant dipolar field (DDF). The strength of the DDF depends on the geometry of the sample and the spatial distribution of the magnetization [1,2,6]. In particular, if the magnetization is modulated by a static magnetic field gradient, the DDF exercises an influence on the evolution of the dipolar-coupled spin ensemble. These phenomena were first observed in experiments on solid ^{3}He [3]. Later experiments demonstrated effects of the DDF in liquid ^{3}He below 100 mK [4] and water at room temperature [5].

The results of these experiments were initially explained within the Bloch theory by introducing the DDF into the Bloch equations [3]. Later, Warren and coworkers [6,7] treated the problem in terms of quantum mechanics. In their model, the measured signal in a CRAZED (COSY revamped by asymmetric Z-gradients echo detection) sequence (Fig. 1) originates from intermolecular multiple-quantum coherences (iMQC) of spins with mutual distance $d = \pi/(\gamma G\tau)$ ("correlation distance," γ = gyromagnetic ratio, G = strength and τ = duration of the magnetic field gradient). The iMQC of positive order N ($N = 1, 2, 3, \ldots$) are generated by an initial rf pulse and are transferred into

* Corresponding author. Fax: +49 6221 42 2531.
E-mail address: p.bachert@dkfz-heidelberg.de (P. Bachert).

1090-7807/$ - see front matter © 2006 Elsevier Inc. All rights reserved.
doi:10.1016/j.jmr.2006.10.011

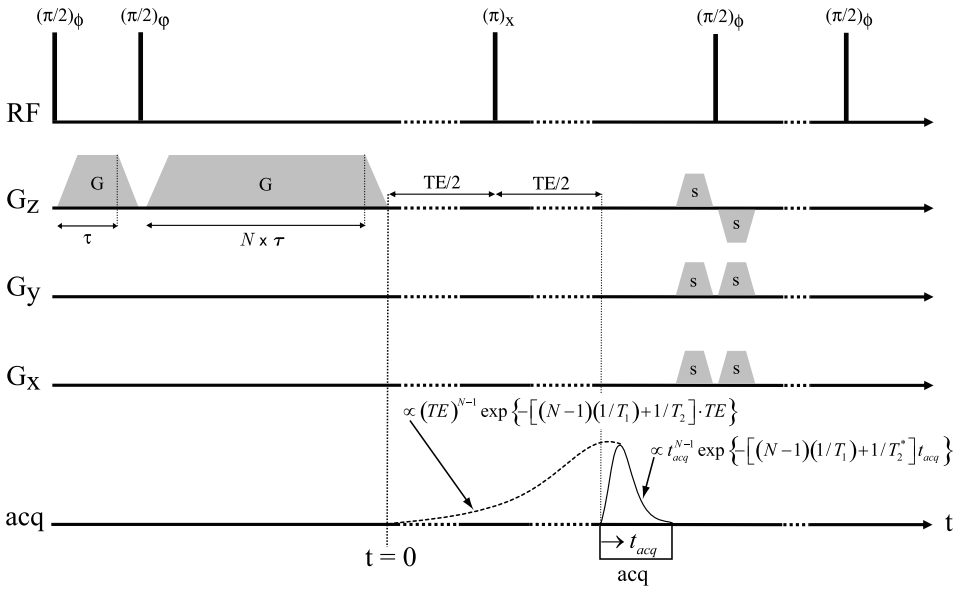

Fig. 1. CRAZED-type pulse sequence. Two-step phase-cycle for selection of iDQC: $\phi = +x, -x$; $\varphi = +x, +x$; acq $= +x, +x$, for selection of iTQC: $\phi = +x, -x$; $\varphi = +x, +x$; acq $= +x, -x$. The gradients s are applied to spoil possible stimulated echoes during the subsequent excitations. Evolution of the echo amplitude as a function of echo time TE (evolution before $t = 0$ is neglected, because $N \cdot \tau \ll$ TE) and measured signal as a function of the detection time t_{acq} are indicated.

observable single-quantum transitions by the combined action of the second rf pulse in the sequence (Fig. 1) and the DDF. The generation of iMQC after a single rf pulse was quite unexpected at that time, but could be explained when it was recognized that the high-temperature approximation of the equilibrium density matrix was insufficient. Jeener [8] proved the equivalence of the semi-classical approach and the quantum-mechanical treatment of the effects of the DDF. In both treatments, the evolution of the transversal magnetization $\Delta M^{\Sigma}(t)$ along the CRAZED-type sequence shown in Fig. 1 is described by $\Delta M^{\Sigma}(t) \propto \xi^{-1} J_N(\xi) \exp(-t/T_2^*)$, where J_N is the Bessel function of order N ($N =$ coherence order) and ξ is a function of time t, longitudinal relaxation time T_1, diffusion constant D, wave vector $k_m = \pi/d$, and the equilibrium magnetization M_0 [9,10,23]. As a consequence, in first-order approximation (effects of diffusion neglected), the signal evolves proportional to $t^{N-1} \exp\{-[(N-1)(1/T_1)+1/T_2^*]t\}$ (Fig. 1) [23].

Robyr and Bowtell [11,12] predicted diffraction-like behavior of the signal generated by the DDF for periodic magnetization distributions. Later, a quantum-mechanical theory was developed to describe this phenomenon [13]: The diffraction pattern depends on the modulation wave length $\lambda_m = 2\pi/k_m$ caused by the applied linear magnetic field gradient and the characteristic wave length $\lambda_s = 2\pi/k_s$ of the periodic structure. The proposed diffraction pattern was observed in experiments on periodic structures [13,20]. It is speculated that NMR diffraction resulting from the DDF could provide a contrast mechanism sensitive to structural properties of heterogeneous samples.

The purpose of our study was to investigate this type of NMR diffraction at lower magnetic field strengths, by means of phantom experiments on a 1.5-T whole-body MR tomograph. Alternative to the quantum-mechanical approach [13], we calculate, on the basis of the semi-classical Bloch equation of motion developed by Robyr and Bowtell [11], the signal in periodic structures expected from the action of the DDF in a CRAZED-type pulse sequence that selects N-quantum coherence. The resulting diffraction conditions for arbitrary N yields insight into the process of signal formation. To our knowledge, this is the first detection of diffraction effects resulting from the DDF in this low magnetic field.

2. Theory

The dipole–dipole coupling between two spins i and j in a static magnetic field B_0 is proportional to $(3\cos^2\theta_{ij} - 1)/r_{ij}^3$, where θ_{ij} is the azimuthal angle between the internuclear vector $\vec{r}_{ij}$ and B_0. In liquid phase, $\vec{r}_{ij}$ will point in all spatial directions during the time scale of the experiment, because of rapid Brownian molecular tumbling motion. Therefore, the isotropic average is $\langle 3\cos^2\theta_{ij} - 1\rangle = 0$ and the net dipole–dipole coupling vanishes. However, this is only true for close spin pairs, while this averaging is ineffective for spins separated by more than the distance molecules can move by diffusion during the experiment ($\sim$10 μm for H_2O) [6].

The residual long-range dipolar couplings can lead to observable effects which have been explained semi-classically by introducing into the Bloch equations the DDF by means of the magnetic induction $\vec{B}_d(\vec{r})$ [3]

$$\vec{B}_d(\vec{r}) = \frac{\mu_0}{4\pi} \int_{-\infty}^{\infty} d^3r' \frac{3\cos^2\theta_{rr'} - 1}{2\left|\vec{r} - \vec{r}'\right|^3} [\vec{M}(\vec{r}') - 3M_z(\vec{r}')\cdot\hat{z}]. \quad (1)$$

Here, $\hat{z}$ = unit vector in the direction of the static field $\vec{B}_0$, μ_0 = vacuum permeability, M_z = longitudinal component of the magnetization $\vec{M}(\vec{r}')$ at point $\vec{r}'$.

We examine diffraction-like phenomena expected for periodic magnetization distributions using the theory developed by Robyr and Bowtell [11]. This formalism is only applicable, if the DDF generates a small-phase perturbation of the transverse magnetization during the evolution time t, i.e., $\gamma B_d t = \omega_d t \ll 1$ rad. For small t, the transversal magnetization $\Delta M^{\Sigma}(\vec{r},t)$ generated by the DDF is, [12]

$$\begin{aligned}\Delta\vec{M}^{\Sigma}(\vec{r},t) &= \vec{M}(\vec{r},t) - \vec{M}(\vec{r},0)\\ &\approx [\gamma \vec{M}(\vec{r},0) \times \vec{B}_d(\vec{r})]t. \end{aligned} \tag{2}$$

Consider the evolution of an ensemble of magnetically equivalent spins in the rotating frame in the presence of B_0 (along the z axis) and the DDF, neglecting relaxation effects and static magnetic field inhomogeneities. Under the assumption, that the DDF arises because of a spatial modulation of the magnetization by means of instantaneously applied gradients, $\Delta M^{\Sigma}(t)$ reads [11]

$$\begin{aligned}\Delta M^{\Sigma}(t) = -\frac{i\gamma\mu_0}{8\pi^3}\int_{-\infty}^{\infty} d^3k \cdot \tilde{P}_2^z(\hat{k}) \cdot \tilde{R}(\vec{k},t)\\ \cdot \tilde{M}^{+}(\vec{k},0)\tilde{M}_z^{*}(\vec{k},0),\end{aligned} \tag{3}$$

where

$$\tilde{M}^{+}(\vec{k},0) = \sum_{n=-\infty}^{\infty} a_n \tilde{M}_0(\vec{k} - n\vec{k}_m^{+}), \tag{4}$$

$$\tilde{M}_z(\vec{k},0) = \sum_{p=-\infty}^{\infty} b_p \tilde{M}_0(\vec{k} - p\vec{k}_m^{z}), \tag{5}$$

$$M^{+}(\vec{r},0) = \sum_{n=-\infty}^{\infty} a_n M_0(\vec{r}) e^{in\vec{k}_m^{+}\cdot\vec{r}}, \tag{6}$$

$$M_z(\vec{r},0) = \sum_{p=-\infty}^{\infty} b_p M_0(\vec{r}) e^{ip\vec{k}_m^{z}\cdot\vec{r}}, \tag{7}$$

are the magnetization distributions at time $t = 0$ in transversal and longitudinal direction in reciprocal and Cartesian space, respectively, and k_m^{+} and k_m^{z} are discrete wave vectors. The dipole–dipole coupling is reflected in the second-order Legendre polynomial

$$\tilde{P}_2^z(\hat{k}) = \frac{3(\hat{k}\cdot\hat{z})^2 - 1}{2} \tag{8}$$

and

$$\tilde{R}(\vec{k},t) = \frac{1 - e^{-2\vec{k}^2 Dt}}{2\vec{k}^2 D} \tag{9}$$

takes into account unrestricted diffusion (D = diffusion constant, $\hat{k} = \frac{\vec{k}}{|\vec{k}|}$).

We extend the semi-classical approach of Ref. [11] and calculate the diffraction conditions for a periodic structure in a CRAZED-type experiment (Fig. 1) that selects iMQC of order $N \geqslant 0$ ($N = 0, 1, 2, 3, \ldots$). The spatial modulation of the magnetization is created by the sequence: $(\pi/2)_y - G(\tau) - (\pi/2)_y - G(N\cdot\tau)$. The first $(\pi/2)$ pulse creates transversal magnetization which is modulated in space by the magnetic field gradient $G(\tau)$ of duration τ:

$$M^{+}(\vec{r}) = M_x(\vec{r}) + iM_y(\vec{r}) = M_0(\vec{r}) e^{i\vec{k}_m\cdot\vec{r}}, \tag{10}$$

where $\vec{k}_m = \gamma \vec{G}\tau$. After the second $(\pi/2)$ pulse and the gradient $G(N\cdot\tau)$, at time $t = 0$

$$M^{+}(\vec{r},0) = \frac{1}{2}M_0(\vec{r})\left(e^{i(1+N)\vec{k}_m\cdot\vec{r}} - e^{-i(1-N)\vec{k}_m\cdot\vec{r}}\right), \tag{11}$$

$$M_z(\vec{r},0) = -\frac{1}{2}M_0(\vec{r})\left(e^{i\vec{k}_m\cdot\vec{r}} + e^{-i\vec{k}_m\cdot\vec{r}}\right). \tag{12}$$

The transverse magnetization generated by the DDF (Eq. 3) can be calculated for the specific magnetization distributions Eq. (11) and Eq. (12): Eq. (6) with $k_m^{+} = k_m$, $a_{(1+N)} = 1/2$, and $a_{-(1-N)} = -1/2$ yields Eq. (11), and Eq. (7) with $k_m^{z} = k_m$, $b_1 = -1/2$, and $b_{-1} = -1/2$ yields Eq. (12). Inserting in Eq. (3) and neglecting diffusion ($D \to 0 \Rightarrow \tilde{R}(\vec{k},t) \to t$) gives

$$\begin{aligned}\Delta M^{\Sigma}(t) = \frac{i\gamma\mu_0}{32\pi^3}t \cdot \int_{-\infty}^{\infty} \tilde{P}_2^z(\hat{k}) \cdot [\tilde{M}_0(\vec{k} - (1+N)\vec{k}_m)\tilde{M}_0^{*}(\vec{k} + \vec{k}_m)\\ + \tilde{M}_0(\vec{k} - (1+N)\vec{k}_m)\tilde{M}_0^{*}(\vec{k} - \vec{k}_m)\\ - \tilde{M}_0(\vec{k} + (1-N)\vec{k}_m)\tilde{M}_0^{*}(\vec{k} + \vec{k}_m)\\ - \tilde{M}_0(\vec{k} + (1-N)\vec{k}_m)\tilde{M}_0^{*}(\vec{k} - \vec{k}_m)]d^3k.\end{aligned} \tag{13}$$

As a consequence of the employed approximations (small t, Eq. (2), $D \to 0$) $\Delta M^{\Sigma}(t)$ depends linearly on time.

Considering $\Delta M^{\Sigma}(t)$ (Eq. 13) in the laboratory frame and taking T_2^{*} relaxation into account, we obtain the line shape

$$\Delta M^{\Sigma}(\omega) \propto \left(\frac{1}{\frac{1}{(T_2^{*})^2} + (\omega_0 - \omega)^2} - \frac{2(\omega_0 - \omega)^2}{\left(\frac{1}{(T_2^{*})^2} + (\omega_0 - \omega)^2\right)^2}\right), \tag{14}$$

which is non-Lorentzian because of the factor t.

According to Ref. [11], in a periodic structure with characteristic wave vector k_s, constructive interference can occur if the shift of the centers in k-space ($\vec{k} = 0$) of the functions $\tilde{M}_0(\vec{k} - (1+N)\vec{k}_m)\tilde{M}_0^{*}(\vec{k} \pm \vec{k}_m)$ and $\tilde{M}_0(\vec{k} + (1-N)\vec{k}_m)\tilde{M}_0^{*}(\vec{k} \pm \vec{k}_m)$ in Eq. (13) is a multiple of $\vec{k}_s$. This condition corresponds to four relations

$$|-(1+N)+1|\vec{k}_m = l\vec{k}_s, \tag{15}$$

$$|-(1+N)-1|\vec{k}_m = l\vec{k}_s, \tag{16}$$

$$|(1-N)+1|\vec{k}_m = l\vec{k}_s, \tag{17}$$

$$|(1-N)-1|\vec{k}_m = l\vec{k}_s, \tag{18}$$

where $l = \pm1, \pm2, \pm3, \ldots$ (Note, that the direction of the shift in k-space has no relevance in this case). Using the

correlation distance $d = \pi/k_m$, Eqs. (16) and (17) yield the diffraction condition

$$d_1 = \frac{|2 \pm N|}{l} \frac{\pi}{|\vec{k}_s|} \cdot \left(\frac{\vec{k}_m}{|\vec{k}_m|} \cdot \frac{\vec{k}_s}{|\vec{k}_s|} \right). \tag{19}$$

and Eqs. (15) and (18) yield

$$d_2 = \frac{|N|}{l} \frac{\pi}{|\vec{k}_s|} \cdot \left(\frac{\vec{k}_m}{|\vec{k}_m|} \cdot \frac{\vec{k}_s}{|\vec{k}_s|} \right). \tag{20}$$

Eq. (19) was found previously by the quantum-mechanical treatment of the problem [13].

Eqs. (19) and (20) are also valid for the case $N < 0$. Negative coherence orders can be selected experimentally by application of a negative second gradient in the pulse sequence in Fig. 1.

A particular case is the intermolecular double-quantum coherence (iDQC) CRAZED experiment ($N = \pm 2$), where a continuous signal upon variation of k_m is predicted [11].

For $N = 2$ the last term in Eq. (13) reads $|\tilde{M}_0(\vec{k} - \vec{k}_m)|^2$; for $N = -2$ the first term in Eq. (13) reads $|\tilde{M}_0(\vec{k} + \vec{k}_m)|^2$. Integration of these functions yields the same result different from zero. The integrals of the other terms, which oscillate strongly, are much smaller. According to Eq. (20) these terms exhibit constructive interference when the distance is $d_2 = \frac{2\pi}{l|\vec{k}_s|}$. Therefore, the signal of the iDQC experiment comprises a continuous signal [11] and a smaller superimposed diffractive component. This agrees with results of iDQC CRAZED experiments with travertine [14], tightly packed glass beads [15,16], trabecular bone [15] and arrays of glass capillaries [18,19].

Pure diffractive signals are only observed in CRAZED experiments on periodic structures that select iMQC with coherence order $N \neq 2$. Since preparation of coherences of order $N = 0$ or $N = \pm 1$ is difficult because of residual FID signal or simultaneous spin echo formation, we focused on triple-quantum coherence (iTQC, $N = \pm 3$) experiments.

The signal origin was verified by reference to the characteristic angular dependence of the dipolar interaction given by $\tilde{P}_2^z(\hat{k})$.

Assume that the extension of the region where the magnetization is different from zero is L. When a gradient is applied such that $|k_m| \geqslant \frac{2\pi}{L}$, the major contribution of $\tilde{M}_0(\ldots) \cdot \tilde{M}_0^*(\ldots)$ in Eq. (13) is located along the direction $\pm k_m$. Hence, in the limit of strong gradients

$$\tilde{P}_2^z(\hat{k}) \to \tilde{P}_2^z\left(\pm \frac{\vec{k}_m}{|\vec{k}_m|} \right) = \frac{3\left(\pm \frac{\vec{k}_m}{|\vec{k}_m|} \cdot \hat{z} \right)^2 - 1}{2} = \frac{3\cos^2 \Theta - 1}{2}, \tag{21}$$

where Θ is the angle between $\vec{B}_0 = B_0 \cdot \hat{z}$ and the direction of the gradient k_m. For $\Theta \approx 54°$ (magic angle), no signal is expected.

3. Material and methods

Experiments were performed on a clinical 1.5-T whole-body MR scanner (Magnetom VISION®; Siemens AG, Medical Solutions, Erlangen, Germany) using a phantom that contained a bundle of approx. 100 tightly packed glass micro-capillaries (o.d. = [1 ± 0.05]mm, i.d. = [0.58 ± 0.05]mm) in a plastic beaker (i.d. = 20 mm) filled with an aqueous solution of $NiSO_4 \cdot 6H_2O$ (1,25 g/l). The capillaries were open at both ends, thus water was inside and outside the capillaries (total ca. 100 ml). Data were acquired by means of a flexible coil (usually applied to MRI of the legs) wrapped around the phantom.

Signals originating from iDQC and iTQC were obtained by the CRAZED-type pulse sequence shown in Fig. 1. In order to minimize unspecific echo contamination of the signal, a two-step phase-cycling scheme according to Ref. [21] was implemented. To avoid stimulated echoes during the subsequent excitations, a (π/2)-pulse surrounded by spoiler gradients was applied immediately after signal acquisition.

The transverse magnetization at the end of the second gradient evolves during the echo delay TE. Signal detection was started after TE = 100 ms, because for this TE we observed maximum signal in experiments on unstructured samples filled with the same aqueous $NiSO_4$ solution.

The magnitude spectrum obtained in iDQC and iTQC experiments was integrated and the integral I was employed as a measure of the transversal magnetization ΔM^{Σ} generated by the DDF. All calculations were performed with ORIGIN® (OriginLab Corporation, Northampton, MA, USA). For calculation of the signal-to-noise ratio (s/n), noise was estimated from peak-free regions.

To study the dependence of ΔM^{Σ} detected in the iMQC CRAZED experiment on the correlation distance d, the echo was measured by incrementing the gradient duration τ from 0.3 to 3 ms (79 steps) for the iDQC, and τ from 0.4 ms to 2.5 ms (85 steps) for the iTQC experiment. The different incrementation resulted from specific properties of sequence programming at the tomograph. With TR = 5 s and NEX = 24 the total measurement time was 180 min. Measurements for the particular coherence order N were performed with the same receiver settings.

iDQC and iTQC experiments were performed with vector $\vec{c}$ (= longitudinal axis of the bundle of capillaries) parallel and perpendicular to the direction of the gradient. According to Eqs. (19) and (20), no diffractive signal is expected for the case $\vec{c} \,\|\, \vec{k}_m (\vec{k}_s \perp \vec{k}_m)$. The relaxation times measured by inversion recovery and spin-echo MRI sequences were $T_1 = (304 \pm 2)$ms and $T_2 = (248 \pm 1)$ms, respectively. The effective transverse relaxation time T_2^* of the phantom was measured by a FID experiment with orientations: $\vec{c} \,\|\, \vec{k}_m (\vec{k}_s \perp \vec{k}_m)$ and $\vec{c} \perp \vec{k}_m (\vec{k}_s \| \vec{k}_m)$. To verify

the DDF as the origin of the measured signal, experiments were also performed with $\Theta = 54°$ between $\vec{B}_0$ and $\vec{k}_m$.

4. Results

Fig. 2 shows the resonance signal in the frequency domain obtained in iDQC and iTQC CRAZED experiments together with the theoretical line shape calculated using Eq. (14) with $T_2^* = 15$ ms. (This value was derived from FID experiments at two orientations of the phantom which yielded $T_2^* = 15$ (±1)ms for $\vec{c} \perp \vec{k}_m$ and $T_2^* = 18$ (±2) ms for $\vec{c} \parallel \vec{k}_m$). The observed shape is non-Lorentzian and asymmetric. The s/n in Fig. 2 is about 250 for the iDQC and about 30 for the iTQC signal.

Fig. 3 shows the result of an iDQC CRAZED experiment with two gradient strengths G of 10 and 12.5 mT/m and increasing duration τ of the gradient pulse corresponding to a reduction of the correlation distance d. The gradient was parallel to $\vec{B}_0$ ($\Theta = 0°$). The intensities change continuously as a function of τ without distinct peaks. For the larger G an attenuation of the signal is observed when τ is increased.

Fig. 3 also shows the result of an iDQC CRAZED experiment with $\Theta = 54°$ and $G = 12.5$ mT/m. The experiment was repeated several times, in each case a signal reduction to $\Theta = 0°$ by a factor ~100 was seen. The residual signal for $\Theta = 54°$ in the iDQC and iTQC experiment decreases with larger gradient duration τ. In the iTQC experiment with $\Theta = 54°$ (Fig. 4), the signal shows the same attenuation than the background signal with $\Theta = 0°$. A possible explanation is magnetization that does not originate from the DDF and/or signal contributions from other coherence orders. The peaks observed in the iTQC experiment with $\Theta = 0°$ vanish in the magic angle

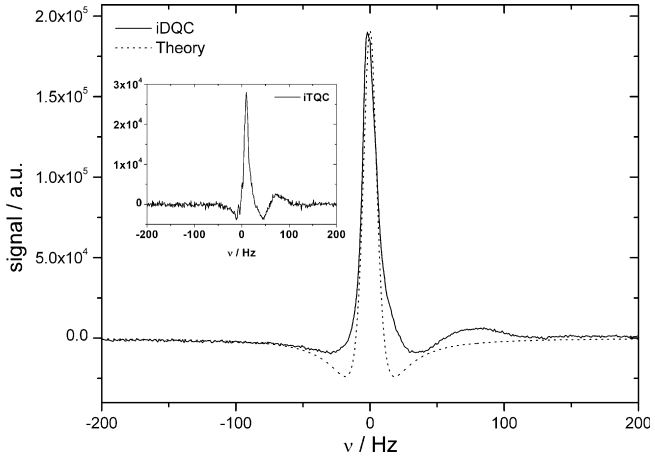

Fig. 2. Line shape (real part) of the CRAZED signal measured on the phantom consisting of water-filled glass capillaries with $\Theta = \sphericalangle(\vec{B}_0, \vec{G}) = 0°$. iDQC signal obtained with $G = 10$ mT/m and $\tau = 0.87$ ms, iTQC signal (insert) obtained with the same G and $\tau = 0.875$ ms (diffraction peak for $d = 1.34$ mm), and theoretical line shape calculated for $T_2^* = 15$ ms (Eq. 14).

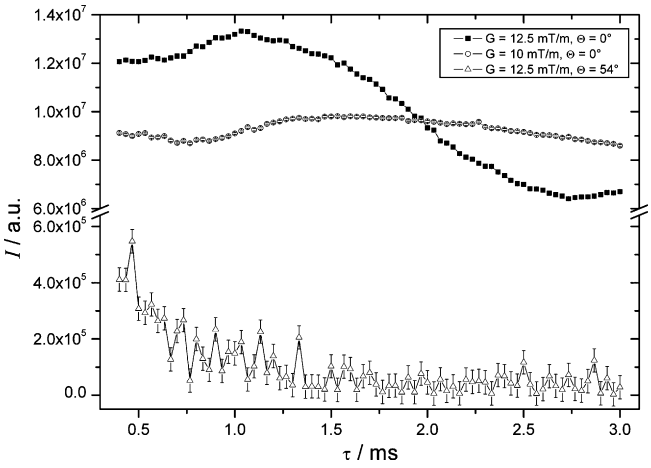

Fig. 3. Integral of the magnitude spectrum I as a function of gradient duration τ observed in an iDQC CRAZED experiment on the phantom consisting of water-filled glass capillaries. Gradient strengths 10 and 12.5 mT/m, both at $\Theta = 0°$, and $G = 12.5$ mT/m at $\Theta = 54°$ were applied. Note the different scaling of the ordinate.

experiment which indicates that the DDF is the cause of these diffraction peaks.

Fig. 4 shows results of an iTQC CRAZED experiment on the same phantom. There is a fundamental difference to the iDQC data since now distinct peaks occur. The most prominent of these are marked with the corresponding correlation distance $d = \pi/(\gamma G\tau)$. The peaks at $d = 2.0$, 1.5, 1.3 and 0.6 mm shift to smaller τ when the gradient strength G is increased. Again, an increasing background signal is observed for small τ. The peaks nearly disappear when the gradient direction $\vec{k}_m$ is at $\Theta = 54°$ with respect to $\vec{B}_0$.

Fig. 5 shows the results of iDQC and iTQC experiments for different orientations of the bundle of capillaries with respect to $\vec{k}_m$. The iTQC experiment yielded distinct peaks when the axis of the bundle was perpendicular to the direction of the gradient. These peaks disappeared when the bundle was parallel to $\vec{k}_m$. For small τ the signal of both coherence orders was lower for that orientation compared to the case where the bundle was perpendicular to $\vec{k}_m$.

5. Discussion

In this study the semi-classical calculations of Robyr and Bowtell [11] were used to derive the diffraction conditions for a periodic magnetization distribution in a CRAZED-type experiment that selects intermolecular N-quantum coherences. Our findings are in agreement with the results of the quantum-mechanical treatment of the problem in Ref. [13].

Diffraction phenomena in NMR have been first demonstrated by Mansfield et al. [22]. The underlying diffraction mechanism they studied does not arise from the DDF.

In previous studies, the dips in the continuous component of the iDQC signal were used to extract structural information [14–17,19]. In the present study, we employed

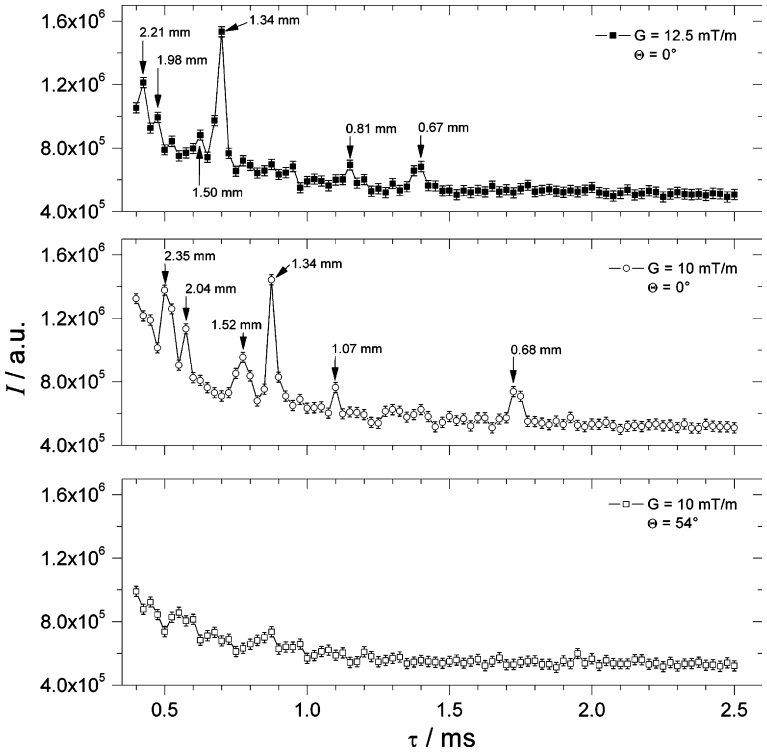

Fig. 4. Integral of the magnitude spectrum I as a function of gradient duration τ observed in an iTQC CRAZED experiment on the capillary phantom with gradient strengths $G = 10$ mT/m and $G = 12.5$ mT/m and orientations $\Theta = 0°$ (top, middle) and $\Theta = 54°$ (bottom). Peaks are labeled by corresponding correlation distances $d = \pi/(\gamma G\tau)$. Duration of each experiment: approx. 3 h.

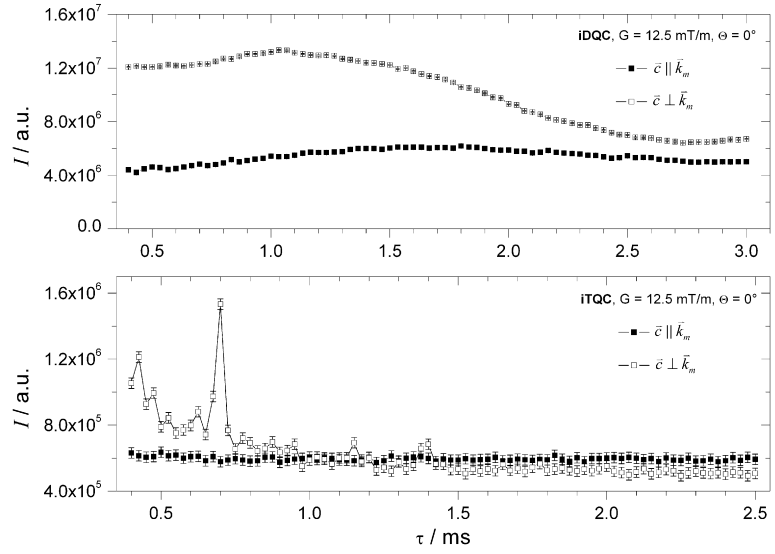

Fig. 5. Integral of the magnitude spectrum I as a function of gradient duration τ for the iDQC and iTQC CRAZED experiments as a function of τ for orientations of the longitudinal axis $\vec{c}$ of the bundle of capillaries parallel (■) and perpendicular (□) to the direction of the magnetic field gradient (iDQC: □ = same data as in Fig. 3, iTQC: □ = same data as in Fig. 4). Only the iTQC experiment yields a distinct peak structure upon variation of τ.

the pure diffractive signal of iTQC CRAZED obtained in experiments at 1.5 T with a heterogeneous liquid system. We could demonstrate the distinctly different signal behavior of iDQC and iTQC CRAZED both theoretically and in phantom experiments. The observed diffraction phenomena of iTQC CRAZED result from residual long-range dipolar interactions between water protons in the capillary system. Our observations agree with findings in similar experiments performed at 4 T [13,18].

The signal origin was verified by measurements with angle $\Theta = 54°$ between the direction of the applied gradient and B_0. The geometrical nature of the diffraction peaks was

verified by two experiments: 1. Measurements with two different strengths of the gradient. 2. Variation of the orientation of the capillaries with respect to the direction of the gradient. The dependence of the angle Θ allows discrimination of signal originating from the presence of the DDF from residual signal from other sources. The observed diffraction peaks could be attributed exclusively to the DDF.

Besides measurements with $\Theta = 54°$, a second method was employed to verify the origin of the diffractive signal. If the longitudinal axis of the bundle of capillaries ($\vec{c}$) is parallel to the direction of the gradient (k_m), the diffractive signal should vanish in the iTQC experiment, while the iDQC signal course should not be affected. This is confirmed by the data in Fig. 5.

Since iMQC are higher-order phenomena, the contamination of the signal of the selected coherence with other signal is a principal problem. Improved coherence selection in CRAZED, particularly at low gradient strengths and/or short gradient durations, is achieved by a phase-cycle consisting of more than two steps [21]. However, because of the extensive measurement time needed (approx. 6 h) this was not applicable here.

We therefore used a two-step phase-cycle to suppress contamination and improve differentiation of coherence orders. However, the two-step phase-cycle can lead to contamination with SQC signal resulting from the second rf pulse. Since T_1 (~300 ms) is much longer than the time interval between the first and second rf pulse ($\approx\tau = 0.3\ldots3$ ms) this contamination is expected to be very small; it is effectively removed by the phase-cycle in the iTQC measurement. On the other hand, the phase-cycle of the iDQC CRAZED sequence is less effective in this respect.

Our first-order approximation of the signal originating from the DDF predicts a non-Lorentzian line shape. The structure of the observed resonances (Fig. 2) qualitatively agrees with the prediction supporting that the DDF is the cause of the signal. We attribute the discrepancies between expected and observed line shape, particularly in the case of iDQC, to residual SQC signal. Since the effectiveness of coherence selection increases with coherence order N (larger phase-shift of unwanted coherences) and the iTQC CRAZED phase-cycle suppresses SQC largely, the iTQC signal is expected to deviate stronger from a Lorentzian than the iDQC signal. This agrees with Fig. 2. (The problem of iMQC line shape will be investigated in a forthcoming paper).

Recently, the line shape problem in CRAZED experiments was analyzed using the quantum-mechanical approach [23]. This treatment included the effects of diffusion and relaxation and also predicted non-Lorentzian line shapes in agreement with our observations in iTQC CRAZED experiments.

In the quantum-mechanical treatment, the phase perturbation caused by the DDF can be estimated from [7]

$$\omega_d \approx 2\tanh\left(\frac{\hbar\omega_0}{2k_BT}\right)\frac{n}{V}\frac{\mu_0\hbar\gamma^2}{6}\left[\frac{3\cos^2\Theta-1}{2}\right], \qquad (22)$$

where n/V = protons per volume, k_B = Boltzmann constant, and T = temperature. With $T = 300$ K, $V = 100$ ml H_2O, $\Theta = 0°$ and $\omega_0 = 2\pi\cdot 63.63\times10^6$ rad/s ($B_0 = 1.5$ T) we obtain $\omega_d \approx 1.1$ rad/s. The average phase $\omega_d \cdot TE$ accumulated by a spin of the sample during the echo delay TE in the sequence in Fig. 1 is 0.11 rad. Thus the employed pulse sequence is compatible to the required condition $\omega_d t \ll 1$ rad. A further reduction of TE was not applicable because of insufficient s/n.

For magnetization distributions that are periodic in space, a distinct difference between iDQC and iTQC CRAZED experiment is expected. A continuous course of the signal as a function of gradient duration τ in the case of iDQC and a diffractive signal behavior for iTQC was observed (Figs. 3 and 4) in agreement with the theoretical prediction. The variation in signal progression observed in Fig. 3 is explained by damping of iDQC (owing to diffusion and shorter T_2^*) and residual SQC signals when the gradient duration τ increases.

In iTQC experiments, with different strengths of the gradient the most distinct diffraction peaks appear at approximately the same correlation distances d (Fig. 4). The parallel shift of the peaks at $d = 1.34$ mm and $d = 0.67$ mm supports the expected relationship between geometrical parameters and peak positions. The observed spectra with distinct diffraction peaks at correlation distances comparable to the size and spacing of the capillaries agree with the regular structure of the bundle of capillaries. Keeping in mind that peak assignments according to the diffraction conditions (19) and (20) must be done carefully, because imperfections and susceptibilities at water/glass surfaces will affect the position of the peaks, we consider the "spectra" obtained at 1.5 T as a fingerprint of the examined geometric structure. Applications of this technique may focus on changes in composition and geometry of periodic structures, which will be detectable by changes in iTQC CRAZED diffraction spectra. The advantage of this method is that heterogeneous liquid systems can be investigated at different length scales simply by changing the strength of the magnetic field gradient. A possible biomedical application of this NMR technique could be studies of the structure of trabecular bone.

References

[1] M.P. Ledbetter, I.M. Savukov, L.S. Bouchard, M.V. Romalis, Numerical and experimental studies of long-range magnetic dipolar interactions, J. Chem. Phys. 121 (2004) 1454–1465.
[2] C.A. Meriles, W. Dong, Indirect detection of nuclear magnetic resonance via geometrically induced long-range dipolar fields, J. Magn. Reson. 181 (2006) 331–335.
[3] G. Deville, M. Bernier, J.M. Delrieux, NMR multiple echoes observed in solid ^{3}He, Phys. Rev. B 19 (1979) 5666–56687.
[4] D. Einzel, G. Eska, Y. Hirayoshi, Multiple spin echoes in a normal Fermi liquid, Phys. Rev. Lett. 53 (1984) 2312–2315.
[5] R. Bowtell, R.M. Bowley, P. Glover, Multiple spin echoes in liquids in a high magnetic field, J. Magn. Reson. 88 (1990) 643–651.
[6] W.S. Warren, W. Richter, A.H. Andreotti, B.T. Farmer, Generation of impossible cross-peaks between bulk water and biomolecules in solution NMR, Science 262 (1993) 2005–2009.

[7] S. Lee, W. Richter, S. Vathyam, W.S. Warren, Quantum treatment of the effects of dipole–dipole interactions in liquid nuclear magnetic resonance, J. Chem. Phys. 105 (1996) 874–900.
[8] J. Jeener, Equivalence between the "classical" and the "Warren" approaches for the effects of long range dipolar couplings in liquid nuclear magnetic resonance, J. Chem. Phys. 112 (2000) 5091–5094.
[9] I. Ardelean, R. Kimmich, Diffusion measurements with the pulsed gradient nonlinear spin echo method, J. Chem. Phys. 112 (2000) 5275–5280.
[10] C. Ramanathan, R. Bowtell, Dynamics of the nuclear magnetic resonance COSY-revamped by asymmetric z-gradients (CRAZED) experiment, J. Chem. Phys. 114 (2001) 10854–10859.
[11] P. Robyr, R. Bowtell, Nuclear magnetic resonance microscopy in liquids using the dipolar field, J. Chem. Phys. 106 (1996) 467–476.
[12] R. Bowtell, P. Robyr, Structural investigations with the dipolar demagnetizing field in solution NMR, Phys. Rev. Lett. 76 (1996) 4971–4974.
[13] X.P. Tang, C.L. Chin, L.S. Bouchard, F.W. Wehrli, W.S. Warren, Observing Bragg-like diffraction via multiple coupled nuclear spins, Phys. Lett. A 326 (2004) 114–124.
[14] S. Capuani, M. Alesiani, F.M. Alessandri, B. Maraviglia, Characterisation of porous media structure by non linear NMR methods, Magn. Reson. Imag. 19 (2001) 319–323.
[15] S. Capuani, F. Curzi, F.M. Alessandri, B. Maraviglia, Characterisation of trabecular bone by dipolar demagnetizing field MRI, Magn. Reson. Med. 46 (2001) 683–689.
[16] F.M. Alessandri, S. Capuani, B. Maraviglia, Multiple spin echoes in heterogeneous systems: physical origins of the observed dips, J. Magn. Reson. 156 (2002) 72–78.
[17] G.D. Charles-Edwards, G.S. Payne, M.O. Leach, A. Bifone, Contrast mechanisms in intermolecular double quantum coherence imaging: a warning, Proc. Intl. Soc. Magn. Reson. Med. 10 (2002) 614.
[18] C. Chin, X. Tang, L. Bouchard, W.S. Warren, F.W. Wehrli, NMR diffraction revisited with a modified CRAZED double quantum imaging sequence, Proc. Intl. Soc. Magn. Reson. Med. 11 (2003) 803.
[19] S. Capuani, M. Alesiani, R.T. Branca, B. Maraviglia, New openings for porous systems research from intermolecular double-quantum NMR, Solid State Nucl. Magn. Reson. 25 (2004) 153–159.
[20] P.L. Sousa, D. Gounot, D. Grucker, Observation of diffraction-like effects in multiple spin echo (MSE) experiments in structured samples, C. R. Chimie 7 (2004) 311–319.
[21] E.D. Minot, P.T. Callaghan, N. Kaplan, Multiple echoes, multiple quantum coherence, and the dipolar field: demonstrating the significance of higher order terms in the equilibrium density matrix, J. Magn. Reson. 140 (1999) 200–205.
[22] P. Mansfield, P.K. Grannell, "Diffraction" and microscopy in solids and liquids by NMR, Phys. Rev. B 12 (1975) 3618–3634.
[23] B. Zheng, Z. Chen, S. Cai, J. Zhong, C. Ye, Theoretical formalism and experimental verification of line shapes of NMR intermolecular multiple-quantum coherence spectra, J. Chem. Phys. 123 (2005) 74317–74324.